Energetics, Kinetics, and Product Distributions of the Reactions of Ozone with Ethene and 2,3-Dimethyl-2-butene

M. Olzmann,*,† E. Kraka,‡ D. Cremer,‡ R. Gutbrod,§ and S. Andersson‡

Institut für Physikalische Chemie der Universität Halle-Wittenberg, FB Chemie Merseburg, D-06099 Halle, Germany; Department of Theoretical Chemistry, University of Göteborg, Kemigården 3, S-41296 Göteborg, Sweden; and Institut für Physikalische Chemie der Universität Kiel, Ludewig-Meyn-Strasse 8, D-24098 Kiel, Germany

Received: May 20, 1997; In Final Form: September 23, 1997[⊗]

A detailed kinetic analysis of the complex reaction systems arising from the ozonolysis of C_2H_4 and $(CH_3)_2C{=}C(CH_3)_2$ (TME), respectively, is carried out, using master equations and statistical rate theory. The thermochemical as well as the molecular data required are obtained from CCSD(T)/TZ2P and B3LYP/DZP calculations. It is shown that the primary ozonides are not collisionally stabilized under atmospheric conditions. In the reaction sequence for O_3 + TME, the same is true for $CH_2{=}C(CH_3)OOH$ formed from $(CH_3)_2COO$, which completely dissociates to give OH radicals. However, in this system, a pressure dependence is predicted for the relative branching fractions of the reactions of the Criegee intermediate. Under atmospheric conditions, for both examples, the product yields obtained are in reasonable agreement with experimental results.

1. Introduction

The reactions with ozone represent an important atmospheric sink for biogenic as well as anthropogenic olefines.[1,2] For this reason, many studies over the past four decades have dealt with their kinetic and mechanistic aspects under different points of view. Whereas the overall kinetics for many of these processes is largely known,[2−5] there is still a considerable uncertainty regarding the detailed mechanisms and the corresponding product yields.[6−9] Especially their possible role as a source of OH radicals[9−12] has increased the attention for this class of reactions again.[13−24]

The now widely accepted general mechanism is shown in the following scheme. For the sake of simplicity, we consider the case of a symmetrically substituted monoalkene (compare with Figure 1):

$$R_2C{=}CR_2 + O_3 \rightarrow POZ^* \quad (1)$$

$$POZ^* + M \rightarrow POZ + M \quad (2)$$

$$POZ^* \rightarrow R_2CO^* + R_2COO^* \quad (3)$$

$$R_2CO^* + M \rightarrow R_2CO + M \quad (4)$$

$$R_2COO^* + M \rightarrow R_2COO + M \quad (5)$$

$$R_2COO^* \rightarrow \text{products} \quad (6)$$

$$R_2COO + X \rightarrow \text{products} \quad (7)$$

Here POZ represents the primary ozonide, and an asterisk indicates vibrational and rotational excitation from chemical activation. M is an inert partner for the collisional stabilization and corresponds to the system pressure. The character X denotes any species capable of bimolecular reactions with the Criegee intermediate R_2COO.

From previous experimental and theoretical[2,12−15,23−25] investigations, there is a strong evidence that the most likely unimolecular reaction channels of the Criegee intermediates are (i) formation of a dioxirane with consecutive reactions to yield molecular or free radical products, (ii) formation of an OH radical via H migration in carbonyl oxide and subsequent OO bond rupture either in an one-step reaction as in the case of H_2COO or via a hydroperoxide intermediate as in the case of syn-alkyl substituted carbonyl oxides,[23,24] and (iii) split-off of $O(^3P)$ atoms after intersystem crossing to the lowest triplet state.[25] These points imply that reaction 6 actually consists of three parallel steps (Figure 1):

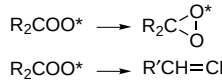

(6a) (6b) (6c)

followed by

$$R'CH{=}CR(OOH)^* \rightarrow R'CH{-}RC{=}O + OH \quad (8a)$$

and

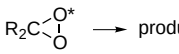

(8b)

In the case R ≡ H, reactions 6b and 8a are replaced by

$$H_2COO^* \rightarrow HCO + OH \quad (6b')$$

because a carbene intermediate HC(OOH) does not exist according to ab initio calculations.[23,24]

The different experimental investigations have highlighted different features of the above mechanism. Because of its important atmospheric implications, many studies deal with the determination of relative OH yields.[6,13,17,19,22,24] For instance, for the reaction $C_2H_4 + O_3$, values of 0.12[17] and 0.08,[22,24] and

* To whom correspondence should be addressed.
† Universität Halle-Wittenberg.
‡ University of Göteborg.
§ Universität Kiel.
⊗ Abstract published in *Advance ACS Abstracts,* November 15, 1997.

S1089-5639(97)01663-0 CCC: $14.00

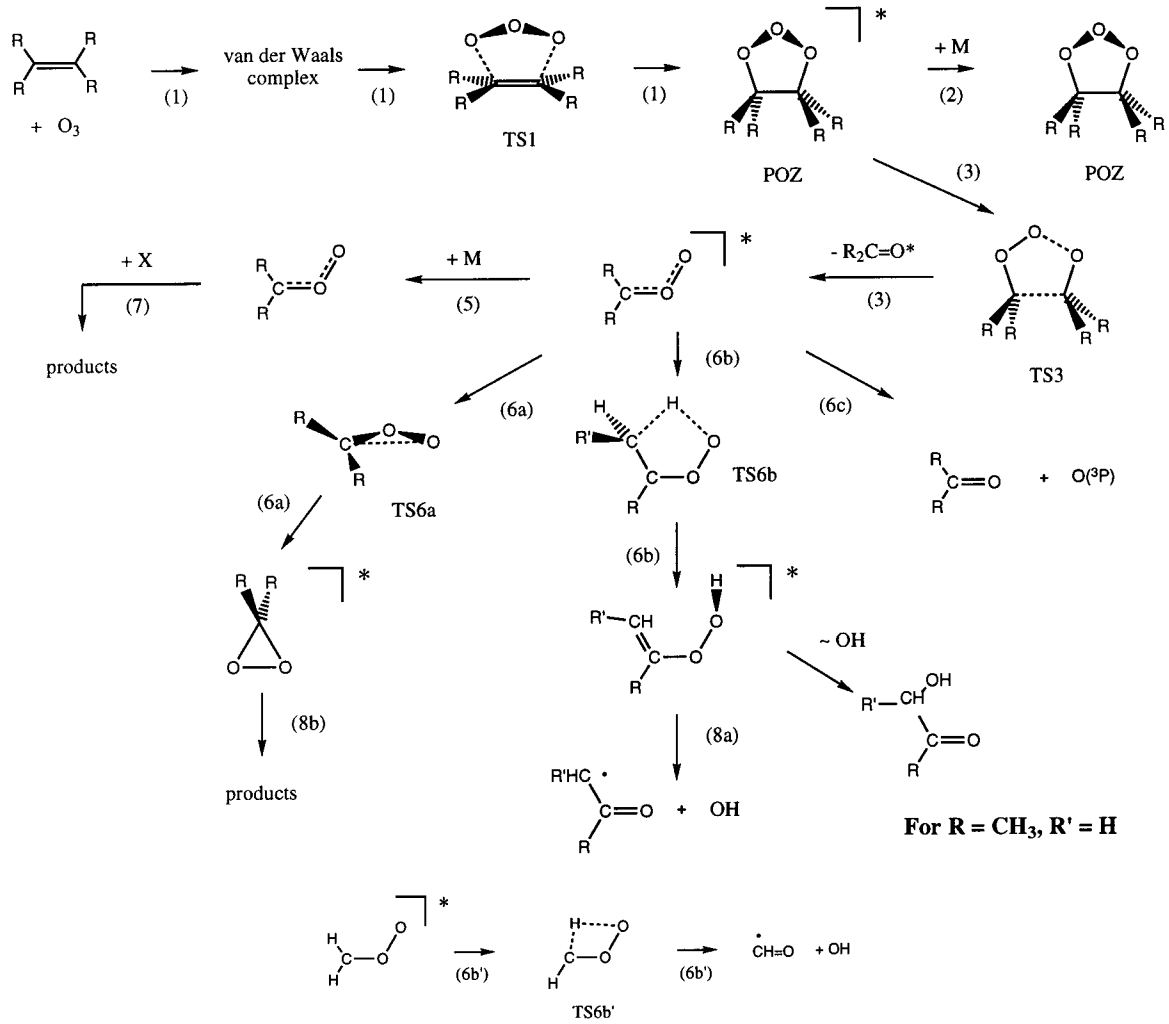

Figure 1. (a) Schematic representation of the mechanism of the ozonolysis of a symmetrically substituted alkene such as tetramethyl ethene (TME). In the case of ethene, Figure 1a applies with the exception of the sequence (6b)−(8a), which is replaced by (b) (6b′). An asterisk denotes vibrational excitation.

for 2,3-dimethyl-2-butene (TME) + O_3 values of 1.0,[19] 0.7,[13] and 0.36[22,24] were found.

Other studies are addressed to the question, what fraction of the chemically activated Criegee intermediates can be stabilized by collisions under atmospheric conditions.[26,27] Here, in good agreement, values between 0.35 and 0.40 for the system O_3 + C_2H_4 were determined independently by several authors.[26,28−30] Moreover, in ref 27, three different fractions of H_2COO were distinguished. 20% turned out to be generally stable even at the lowest pressure of this investigation (13 mbar), and it was argued[27] that these Criegee intermediates are already generated in a stable form. Further 20% could be stabilized by increasing the pressure from 13 to 1520 mbar, and the remaining 60% could not be stabilized even at this relatively high pressure. For the reaction O_3 + TME, relative yields of 0.30[13] for the stabilized $(CH_3)_2COO$ were determined.

Martinez et al.[14] estimated the stability of an intermediate hydroperoxide, CH_2=$C(CH_3)OOH$, possibly formed from $(CH_3)_2COO$, using RRK theory. The thermochemistry was estimated using group increments and partly thermochemical data for the system C_2H_4 + O_3. It was concluded that the hydroperoxide should not decompose at pressures as low as 5 mbar. This is in contradiction to experimental results, where even under atmospheric conditions no CH_2=$C(CH_3)OOH$ could be detected.[13] This point was also discussed by Martinez et al.[14] and explained with the possible presence of additional pathways such as isomerization to hydroxyacetone. However, no rate data for these channels could be given.

In view of these numerous approaches, that emphasize largely different features of the mechanism, it is the aim of the present article to develop an appropriate model of the ozonolysis reaction that is based on quantum chemical calculations and statistical rate theory, and that can be used to rationalize the production of varying amounts of OH radicals during the ozonolysis of different alkenes. Within this picture, the differing experimental findings are summarized and quantitatively interpreted from a common point of view. To obtain the thermochemical data as well as the molecular properties required, we characterize the stationary points on the corresponding potential-energy surfaces (PES) by density-functional theory (DFT), Møller−Plesset (MP) methods (in part), and coupled-cluster (CC) methods. Utilizing the results of the quantum chemical calculations, the reactions of ozone with ethene and TME are investigated by carrying out a detailed kinetic analysis. The chemically activated reaction systems are described by a master-equation, employing specific rate coefficients from RRKM theory and from the statistical adiabatic channel model. As a result, lifetimes of several intermediate species under different conditions are derived, and mechanistic consequences relevant to their decomposition are discussed. In the present work, we focus on recent kinetic measurements for the reaction systems ozone/ethene and ozone/TME.[22]

2. Quantum Chemical Calculations

In previous work on the ozonolysis of ethene,[31−35] we have tested Hartree−Fock theory, many-body perturbation theory with the Møller−Plesset perturbation operator (MP), coupled-cluster (CC) theory, and density-functional theory (DFT) to find a reliable but economic method that provides a reasonable description of the various steps of the ozonolysis reaction. These investigations revealed that an accurate description of the ozonolysis of ethene is obtained at the CCSD(T) level using a TZ+2P basis set while other methods, which cover less correlation effects, fail to provide a consistent description of all reaction steps.[23,34,35] However, CCSD(T)/TZ+2P calculations become rather costly when investigating the ozonolysis of higher alkenes such as TME and, therefore, a compromise had to be found in the present work. This was found by using DFT with Becke's three parameter hybrid functional B3LYP and a 6-31G(d,p) basis set.[36,37]

B3LYP/6-31G(d,p) provides reasonable reaction energies and barriers for most of the ozonolysis steps insofar as the calculated B3LYP values are more accurate than those obtained with MP2 theory.[35] As is well-known, DFT fails in the case of van der Waals complexes and loose transition states (TS).[38] For example, energy and geometry of the ozone-ethene van der Waals complex are erroneously predicted by B3LYP and the barrier of the ozone-ethene cycloaddition reaction (TS1, see Figure 1) is calculated to be just 0.2 kcal/mol and, thereby, largely underestimated. On the other hand, it is calculationally feasible to describe both the ethene and the TME ozonolysis at the B3LYP/6-31G(d,p) level of theory and, therefore, this method was used to calculate energies, geometries, and frequencies of all the molecules and TS shown in Figure 1. The corresponding Cartesian coordinates, rotational constants, and harmonic wavenumbers are available as Supporting Information.

Zero-point energy (ZPE) and temperature corrections for $T = 298$ K were calculated by scaling the harmonic B3LYP/6-31G(d,p) frequencies by a factor of 0.963. Calculations have been performed with COLOGNE94,[39] GAUSSIAN 94,[40] and ACES II ab initio programs.[41] ZPE values and temperature corrections were combined with B3LYP reaction energies to obtain reaction enthalpies $\Delta\Delta H_f°$ at 0 and 298 K. Utilizing the experimental heats of formation $\Delta H_f°(0)$ and $\Delta H_f°(298)$ of ozone, ethene, TME, formaldehyde, and acetone (denoted by a star in Table 1)[42] as well as calculated reaction enthalpies $\Delta\Delta H_f°$ at 0 and 298 K, it was possible to derive for each molecule and TS of Figure 1 heats of formation $\Delta H_f°(0)$ and $\Delta H_f°(298)$, which are listed in Table 1 (sets A1 and B1) together with energies, ZPE values, and temperature corrections.

In the case of TS1 (Figure 1), in which B3LYP fails to predict a reasonable geometry and energy, an activation energy of 1.9 kcal/mol relative to the energies of ozone and ethene (2.5 kcal/mol if calculated relative to the energy of the ozone−ethene van der Waals complex; the corresponding enthalpy values are 3.5 and 4.2 kcal/mol) taken from a MP4 investigation[35,43] was used to complement the energetics. The same barrier value was also assumed for the corresponding cycloaddition reaction between ozone and TME although in this case the van der Waals complex is probably more stable and the TS somewhat higher in energy.[44]

To check whether the B3LYP/6-31G(d,p) data provide a consistent description of the various steps of the ozonolysis reaction as described in Figure 1, some of the calculations were repeated at the CCSD(T) level of theory[45] employing a TZ+2P basis set derived from a (11s6p3d/5s3p) [5s3p2d/3s2p] contraction augmented with Cartesian polarization functions.[46] In previous investigations it was shown that CCSD(T)/TZ+2P calculations are rather reliable so that accurate reaction enthalpies can be obtained.[23,34]

Due to the size of the basis set, CCSD(T) calculations were only feasible for the three heavy atom systems so that just the rearrangement possibilities of the carbonyl oxide could be investigated (entries 7−17 in Table 1, set A2). Reaction enthalpies 7 to 15 are 0.5 to 2.3 kcal/mol smaller when calculated at the CCSD(T)/TZ+2P level of theory, which is what one should expect as a difference between DFT and CCSD(T) in these cases. However in the case of 16 and 17, reaction enthalpies differ by 7.6 kcal/mol. The reaction leading from carbonyl oxide to formyl and OH radical is difficult to calculate since it requires the comparison of a closed shell system with two open shell systems where the relative stability of the two radicals may be underestimated because of spin contamination when using an UHF reference function as done in this work. On the other hand, UHF−CCSD(T) is known to lead to only negligible spin contamination in the case of doublet radicals[47] and, therefore, the CCSD(T) reaction enthalpies 16 and 17 should be more reliable than the corresponding DFT values.

The calculated $\Delta H_f°(298)$ value for 16 can directly be compared with the corresponding experimental $\Delta H_f°(298)$, which is 19.2 kcal/mol ($\Delta H_f°(298, OH) = 9.30 \pm 0.3$; $\Delta H_f°(298, HCO) = 9.90 \pm 0.5$ kcal/mol[42]). The DFT result differs by just −2.3 kcal/mol while the difference increases to almost −10 kcal/mol if CCSD(T) energies are used to derive $\Delta H_f°(298)$ values (set A2). Clearly, this is in contradiction to the higher accuracy provided by the CCSD(T) method and suggests that the combination of DFT and CCSD(T) results is problematic. The analysis of heats of formations $\Delta H_f°(298)$ for 1−9 of Table 1 reveals that DFT fails when determining $\Delta H_f°(298)$ of carbonyl oxide. This was calculated to be 30.2 kcal/mol in a CCSD(T) investigation of Cremer and coworkers.[34] Earlier GVB calculations of Harding and Goddard[48] led to a similar value while B3LYP/6-31G(d,p) predicts a value of 22.1 kcal/mol which is 8 kcal/mol smaller. Repeating some of the B3LYP calculations with a 6-311+G(3df,2p) basis set reduces this difference by 4.5 kcal/mol, where the remaining difference may be due to residual spin contamination. Hence, the more reliable $\Delta H_f°$ values can be obtained when using the CCSD(T) value of $\Delta H_f°(7)$ in connection with the B3LYP energies for 1−6 (exception 4: MP4) and the CCSD(T) values for 7−17. If this is done, a $\Delta H_f°(298, 16)$ value of 18.2 kcal/mol is obtained, which differs from the experimental value by just −1 kcal/mol (Table 1, set A3).

The most accurate heats of formation are listed in the last two columns of Table 1 (set A3). We note that the major change in reaction enthalpies due to the use of the CCSD(T) value for $\Delta H_f°(298, 7)$ occurs in the decomposition reaction of ethene POZ, which becomes about 8 kcal/mol more endothermic ($\Delta\Delta H_f°(298)$ increases from 6.6 to 14.7 kcal/mol; Table 1). As is discussed in section 4, this has a negligible influence on the kinetic behavior of the carbonyl oxide.

In view of the results obtained for the ozonolysis of ethene, we have also improved the B3LYP/6-31G(d,p) reaction enthalpies and heats of formation calculated for the ozonolysis of TME (part B of Table 1). This was done by determining the $\Delta H_f°(298)$ value of dimethyldioxirane (entry 28) with the help of the formal reaction c-$(CH_3)_2COO$ + CH_4 → c-CH_2OO + $CH_3CH_2CH_3$ utilizing experimental $\Delta H_f°$ values for methane and propane,[42] the CCSD(T) $\Delta H_f°(298)$ value of dioxirane[34] (see entry 12 of Table 1, set A3) and the calculated reaction enthalpy.

TABLE 1: Energies, Zero-Point Energies and Heats of Formation Calculated at the B3LYP/6-31G(d,p) and CCSD(T)/[5S3P2D/3S2P] Level of Theory

molecule	energy E^a	ref	ΔE	ZPE	ΔE + ZPE	$-\Delta$	$\Delta H_f°(0)$	$\Delta H_f°(298)$	$\Delta H_f°(0)^d$ final	$\Delta H_f°(298)^d$ final
A. Ozonolysis of ethene							set A1		set A2	
B3LYP/6-31G(d,p)										
1) O_3	−225.40645			4.5		0.6	34.7*	34.1*	34.7*	34.1*
2) $H_2C{=}CH_2$	−78.59381			30.9		2.0	14.6*	12.5*	14.6*	12.5*
3) 1 + 2	−304.00026		0	35.4	0	2.7	49.3*	46.6*	49.3*	46.6*
4) TS1	*b*	3	1.9	37.0	3.5	3.6			52.8	49.2
5) Ethene POZ	−304.09949	3	−62.3	40.1	−57.3	4.2	−8.0	−12.2	−8.0	−12.2
6) TS3	−304.06525	5	21.5	37.9	19.2	4.0	11.1	7.1	11.1	7.1
7) H_2COO	−189.57989			18.9		1.7	23.8	22.1	31.9	30.2
8) $H_2C{=}O$	−114.50320			16.1		0.9	−26.8*	−27.7*	−26.8*	−27.7*
9) 7 + 8	−304.08312	5	10.3	35.0	5.2	2.6	−3.0	−5.6	5.1	2.5
10) TS6a	−189.54566	7	21.5	17.9	20.5	2.2	44.3	42.1	50.1	47.9
11) 8 + 10	−304.04886	9	21.5	34.0	20.5	3.1	17.5	14.4	23.3	20.2
12) c−H_2COO	−189.61829	7	−24.1	19.7	−24.3	1.1	−0.5	−1.6	7.1	6.0
13) 8 + 12	−304.12149	9	−24.1	35.8	−24.3	2.0	−27.3	−29.3	−19.7	−21.7
14) TS6b	−189.52430	7	34.9	15.7	31.7	1.7	55.5	53.8	62.7	61.0
15) 8 + 14	−304.02750	9	34.9	31.8	31.7	2.6	28.7	26.1	35.9	33.3
16) HCO + OH	−189.58021	7	−0.2	13.0	−6.1	0.8	17.7	16.9	19.0	18.2
17) 8 + 16	−304.08341	9	−0.2	29.1	−6.1	1.7	−9.1	−10.8	−7.8	−9.5
CCSD(T)/[5s3p2d/3s2p]^c							set A2			
7) H_2COO	−189.32044			18.9		1.7	23.8	22.1		
10) TS6a	−189.28984	7	19.2	17.9	18.2	2.2	42.0	39.8		
11) 8 + 10		9	19.2	34.0	18.2	3.1	15.2	12.1		
12) c−H_2COO	−189.36124	7	−25.6	19.7	−24.8	1.1	−1.0	−2.1		
13) 8 + 12		9	−25.6	35.8	−24.8	2.0	−27.8	−29.8		
14) TS6b	−189.26626	7	34.0	15.7	30.8	1.7	54.6	52.9		
15) 8 + 14		9	34.0	31.8	30.8	2.6	27.8	25.2		
16) HCO + OH	−189.33287	7	−7.8	13.0	−13.7	0.8	10.1	9.3		**19.2** (exp)
17) 8 + 16		9	−7.8	29.1	−13.7	1.7	−16.7	−18.4		**−8.5** (exp)
B. Ozonolysis of TME							set B1		set B2	
B3LYP/6-31G(d,p)										
18) TME	−235.87358			99.2		7.8	−8.5	−16.3*	−8.5	−16.3*
19) O_3 + TME	−461.28003		0	103.7	0	8.4	26.2	17.8	26.2	17.8
20) TS1	*b*	19			3.5	9.3			29.7	20.4
21) TME POZ	−461.38159	19	−63.7	107.8	−59.6	10.1	−33.4	−43.5	−33.4	−43.5
22) TS3	−461.35625	21	15.9	105.7	13.8	9.9	−19.6	−29.5	−19.6	−29.5
23) $(CH_3)_2COO$	−268.24593			52.8		4.6	−7.7	−12.3	−1.9	−6.5
24) $(CH_3)_2C{=}O$	−193.16421			50.6		3.9	−48.0*	−51.9*	−48.0*	−51.9*
25) 23 + 24	−461.41014	21	−17.9	103.4	−22.3	8.5	−55.7	−64.2	−49.9	−58.4
26) TS6a	−268.21000	23	22.5	52.0	21.7	4.9	14.0	9.1	17.1	12.2
27) 24 + 26	−461.37421	25	22.5	102.6	21.7	8.8	−34.1	−42.9	−30.9	−39.7
28) c-$(CH_3)_2COO$	−268.27749	23	−19.8	53.4	−19.2	4.8	−26.9	−31.7	−22.3	−27.1
29) 24 + 28	−461.44162	25	−19.8	104.0	−19.2	8.7	−75.0	−83.7	−70.3	−79.0
30) TS6b	−268.21877	23	17.0	50.6	14.8	5.0	7.1	2.1	12.1	7.1
31) 24 + 30	−461.38298	25	17.0	101.2	14.8	8.9	−41.0	−49.8	−35.9	−44.8
32) $H_2C{=}C(Me)OOH$	−268.26753	23	−13.6	53.1	−13.3	4.4	−21.0	−25.4	−15.2	−19.6
33) 24 + 32	−461.43174	25	−13.6	103.7	−13.3	8.3	−69.1	−77.4	−63.2	−71.5
34) $H_2C(Me)CO$ + OH	−268.23072	23	9.5	47.7	4.4	2.6	−3.3	−5.9	6.2	**3.6** (exp)
35) 24 + 34	−461.39493	25	9.5	98.3	4.4	6.5	−51.4	−57.5	−41.8	**−48.3** (exp)

[a] Absolute energies in hartree, relative energies, zero-point energies (ZPE), thermal corrections Δ, and heats of formation in kcal/mol. ZPE values and thermal corrections Δ have been obtained from B3LYP/6-31G(d,p) frequencies scaled by a factor of 0.963. Heats of formation at 0 K, $\Delta H_f°(0)$, and at 298 K, $\Delta H_f°(298)$, denoted by a star have been taken from JANAF tables (ref 42a) and were used to derive the other heats of formation in the table. For the definition of transition states (TS), see Figure 1. Dioxiranes are abbreviated as c−H_2COO and c-$(CH_3)_2COO$. [b] At the B3LYP/6-31G(d,p) level, TS1 was not found for the ozonolysis of ethene. The values given are from MP4/6-31G(d,p) and MP2/6-31G(d,p) calculations (see ref 35 and 43). These values have also been assumed for the ozonolysis of TME. [c] Relative energies calculated at the CCSD(T)/[5s3p2d/3s2p] level of theory were used for ΔE and combined with ZPE and thermal corrections calculated at B3LYP/6-31G(d,p). [d] Values are based on CCSD(T) value of the heat of formation of carbonyl oxide (see ref 34) and the CCSD(T)/[5s3p2d/3s2p] results (see text).

In this way, $\Delta H_f°(298, 28) = -27.1$ kcal/mol was obtained for dimethyldioxirane, which in turn was used to calculate $\Delta H_f°(298, 23)$ of the corresponding carbonyl oxide isomer (−6.5 kcal/mol, Table 1). Because of the size of the molecules involved, no CCSD(T)/TZ+2P calculations could be carried out for the ozonolysis of TME. However, it was assumed that CCSD(T) calculations would lead to similar corrections as those found for the ozonolysis of ethene. Hence, the final $\Delta H_f°$ values listed in Table 1 (set B2) for the ozonolysis of TME are based on DFT reaction enthalpies corrected where possible by CCSD(T) results for the ozonolysis of ethene and the CCSD(T) enthalpy of carbonyl oxide. Again, this leads to a major change in the excess energy of dimethylcarbonyl oxide and aceton, which is reduced from 82 (B3LYP) to 76 kcal/mol. Other changes are < 2.3 kcal/mol for the remaining reaction enthalpies.

The data in the last two columns of Table 1 (sets A3 and B2) provide a consistent and reliable description of the energetics of the ozonolysis of ethene and TME. Nevertheless, it is useful to bear in mind that the relative stability of the carbonyl oxides changes by 8 kcal/mol when replacing B3LYP/6-31G(d,p) by CCSD(T)/TZ+2P results.

3. Relative Yields from Statistical Rate Theory

The Master Equation. The kinetic quantities of a chemical activation system can be derived by solving the corresponding master equation.[49−53] If one considers a species, which is formed by a chemical reaction and, subsequently, is subjected to the competition between collisional stabilization and consecutive reactions (decomposition, isomerization), the master equation can be understood as the balance over all gain and loss processes for a given energy level, *i*, of this species:

$$\frac{\mathrm{d}n_i}{\mathrm{d}t} = R_{\mathrm{form}} f_i - \omega n_i + \omega \sum_j P_{ij} n_j - \sum_r k_{ri} n_i \qquad (9)$$

Here n_i is the concentration of the intermediate having internal energy E_i. R_{form} is the overall rate of its formation and f the normalized distribution over the energies E_i, as generated by the formation reaction. The second and the third term describe the collisional depopulation and population, respectively, of the considered level i, with the collision frequency ω and the probabilities P_{ij} for transitions $j \rightarrow i$. The last term represents the consecutive reactions with the specific rate coefficients $k_{ri} = k_r(E_i)$ for the reaction pathway r. Equation 9 can conveniently be written in matrix form.[49,53] Assuming steady-state conditions,[54] $\mathrm{d}n_i/\mathrm{d}t = 0$, one obtains

$$R_{\mathrm{form}} \boldsymbol{F} = [\omega(\boldsymbol{I} - \boldsymbol{P}) + \sum_r \boldsymbol{K}_r] \boldsymbol{N}^s \equiv \boldsymbol{J}\, \boldsymbol{N}^s \qquad (10)$$

where the vector/matrix symbols correspond to the symbols in eq 9, and $\boldsymbol{I}$ denotes the unit matrix. The steady-state population $\boldsymbol{N}^s$ now follows from

$$\boldsymbol{N}^s = R_{\mathrm{form}}\, \boldsymbol{J}^{-1}\, \boldsymbol{F} \qquad (11)$$

and the rate of the reaction r, D_r, is obtained by averaging the rate coefficients k_{ri} over this distribution:

$$D_r = \sum_i (\boldsymbol{K}_r \boldsymbol{N}^s)_i \qquad (12)$$

Here $(X)_i$ stands for the ith diagonal element of the matrix X.

Finally, the desired relative yields are given by

$$\frac{D_r}{R_{\mathrm{form}}} = \sum_i (\boldsymbol{K}_r \boldsymbol{J}^{-1} \boldsymbol{F})_i \qquad (13)$$

and the stabilized fraction, S/R_{form}, follows from the steady-state condition $S/R_{\mathrm{form}} = 1 - \sum D_r/R_{\mathrm{form}}$.

In our calculations, we used a stepladder model[49−52,55] (step size: ΔE_{SL}) for the transition probabilities P_{ij} and Lennard-Jones collision numbers for ω.[56] Energy-transfer parameters for the species of interest in this work with N_2 and O_2 are not known. Thus, the calculations were actually carried out for two different values of ΔE_{SL}, viz. 250 and 500 cm^{-1}. For the Criegee intermediates, these values correspond to average energies transferred per collision of about -100 cm^{-1} and -350 cm^{-1}, respectively.[57] In view of experimentally determined values for organic molecules of comparable size,[58] we believe that our quantities should represent reasonable lower and upper limits for the efficiency of the collisional deactivation in our systems. Moreover, it turned out that, in general, the results are not very sensitive to ΔE_{SL} (see below). The inversion of the tridiagonal matrix $\boldsymbol{J}$ was achieved by standard procedures[59] with a grain size of 10 cm^{-1}.

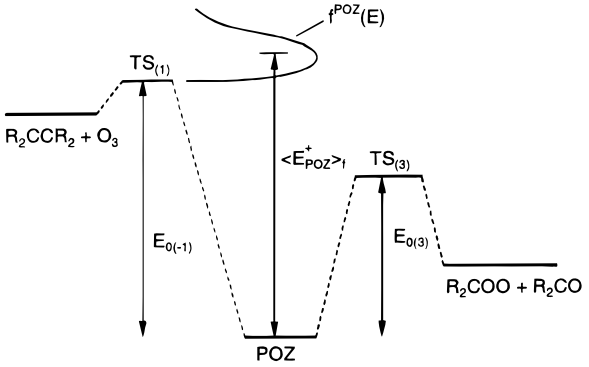

Figure 2. Schematic energy diagram with the nascent population of the primary ozonide. $\mathrm{TS}_{(i)}$ denotes the transition state of reaction i, $E_{0(i)}$ the corresponding threshold energy; for details see text.

Specific Rate Coefficients. The specific unimolecular rate coefficients are calculated by RRKM theory:[49−51,60]

$$k_r(E) = \frac{W_r(E - E_{0(\mathrm{r})})}{h\rho(E)} \qquad (14)$$

with W_r being the sum of states of the transition state for the reaction r and $E_{0(r)}$ the corresponding threshold energy. The symbol h stands for Planck's constant, and ρ represents the density of states of the reactant. The sums and densities of states are determined by counting procedures.[61]

In the case of simple bond breaking, a TS may not exist on the PES as encountered for reaction 8a. Here the specific rate constants are calculated by the statistical adiabatic channel model (SACM),[62] where the sum of states in eq 14 is substituted by the corresponding number of open reaction channels.

Molecular Distribution Functions. A further necessary input quantity for eq 13 is the nascent molecular population $f_i = f(E_i)$. One has to distinguish between three different cases that occur in our systems. The chemically activated species may be formed by (i) an exoergic bimolecular step as in reaction 1, (ii) a unimolecular decomposition of an energized precursor as in reaction 3, or (iii) a unimolecular isomerization step as in reaction 6b.

The input population in the first case can be described by a shifted thermal distribution:[49−51]

$$f^{\mathrm{POZ}}(E) = \frac{W_{\mathrm{POZ}}(E - E_{0(-1)}) \exp[-(E - E_{0(-1)})/k_{\mathrm{B}}T]}{\int_0^\infty W_{\mathrm{POZ}}(\epsilon) \exp(-\epsilon/k_{\mathrm{B}}T)\mathrm{d}\epsilon} \qquad (15)$$

for $E \geqslant E_{0(-1)}$ with the energy being counted from the ground state of the primary ozonide. Here W_{POZ} is the sum of states of the primary ozonide, $E_{0(-1)}$ the threshold energy for the reverse process of reaction 1, and k_{B} represents Boltzmann's constant. The essential features are included in Figure 2.

In the second case, the nascent population can be obtained by assuming statistical energy partitioning between the dissociating fragments. With an overall disposable energy $E^+_{(3)}$, it follows for the input distribution of the Criegee intermediate:[50]

$$f^{\mathrm{R_2COO}}(E) = \frac{\rho_{\mathrm{R_2COO}}(E) W_{\mathrm{R_2CO}}(E^+_{(3)} - E)}{\int_0^{E^+_{(3)}} \rho_{\mathrm{R_2COO}}(\epsilon) W_{\mathrm{R_2CO}}(E^+_{(3)} - \epsilon)\mathrm{d}\epsilon} \qquad (16)$$

with the sums and densities of states as indicated by the subscripts. Here the energy zero is the ground state of R_2COO, and the situation is illustrated in Figure 3.

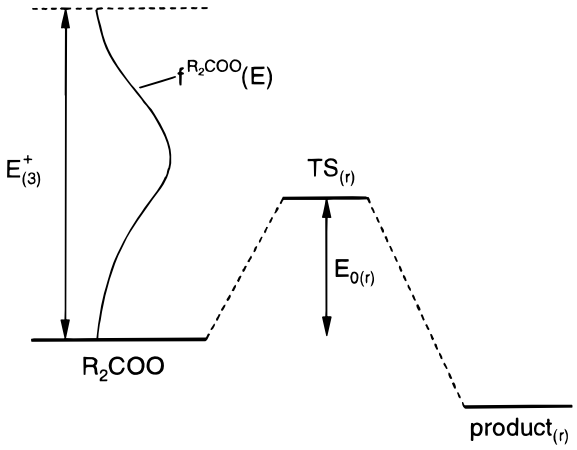

Figure 3. Schematic energy diagram with the nascent population of the Criegee intermediate and the disposable energy $E^+_{(3)}$ in relation to the threshold energy for the unimolecular processes.

Finally, in the third case, the nascent population of RR′C(OOH) generated by reaction 6b is accessible by a steady-state treatment, which results in

$$f^{RR'COOH}(E) = \frac{k_{6b}(E)n^s_{RR'COO}(E)}{\int_{E_{0(6b)}}^{\infty} k_{6b}(\epsilon)n^s_{RR'COO}(\epsilon)\,d\epsilon} \qquad (17)$$

where again the energy is counted from the ground state of R_2COO.

4. Results and Discussions

For the kinetic modeling, calculated enthalpies (Table 1 and Section 2), geometries, and frequencies are utilized. We employ the probably most reliable thermochemical data sets from Table 1 (set A3 and B2, respectively) and discuss consequences of uncertainties in these values separately. The sums and densities of states as well as the specific rate coefficients are calculated for a total angular momentum quantum number of 23 and 55, respectively. These values can be estimated from the combination of the average angular momenta of thermal ensembles of O_3/C_2H_4 and O_3/TME, respectively. All calculations were carried out for a temperature of 298 K.

$C_2H_4 + O_3$. The nascent population of the primary ozonide follows from eq 15. The average energy of this population $<E^+_{POZ}>_f = 62.6$ kcal/mol (see Figure 2). This input distribution is changed into the steady-state distribution, n^s, by collisions and the unimolecular decomposition (see eq 11). The calculated average rate constant toward $H_2COO + H_2CO$ is 9.1×10^{11} s^{-1}. This is large compared to a collision frequency of 8.8×10^9 s^{-1} at 1013 mbar and indicates that there is practically no stabilization of the primary ozonide under these conditions. The normalized steady-state distribution differs little from $f^{POZ}(E)$ as can be seen from the corresponding average energy $<E^+_{POZ}>_n = 62.5$ kcal/mol. The master equation with $\Delta E_{SL} = 500$ cm^{-1} predicts a stabilized fraction of 0.05% at 100 bar and 35% at 1000 bar.

The average energy difference $E^+_{(3)} = <E^+_{POZ}>_n - E_{0(3)} = 43.3$ kcal/mol is available for partitioning between H_2COO and H_2CO in the dissociation reaction. The resulting distribution $f^{H_2COO}(E)$ follows from eq 16 and is shown in Figure 4. The average energies are: H_2COO: 24.9, H_2CO: 14.1, and relative translation: 4.3 kcal/mol. From $f^{H_2COO}(E)$ and the corresponding specific rate constants, which are also included in Figure 4, the relative yields of dioxirane (D_{6a}/R_{form}), OH ($D_{6b'}/R_{form}$) and the stabilized Criegee intermediate (S/R_{form}) are accessible via eq 13. The results for two different pressures are shown in Table 2. As was already mentioned above, the relative fractions in this pressure range are only little dependent on ΔE_{SL}.

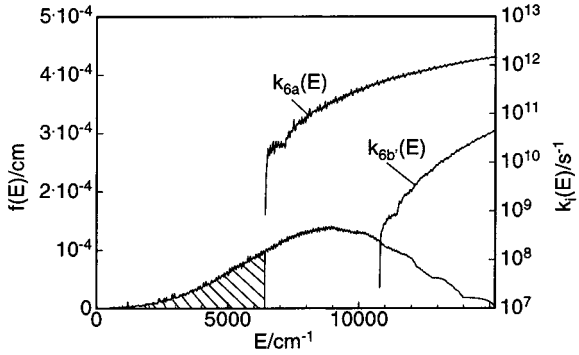

Figure 4. Nascent population of H_2COO and specific rate coefficients for the consecutive reactions. The hatched area represents the part of the population that is initially stable. The coarse structure in the distribution at high energies is due to energy quantization in the complementary molecule formaldehyde at low energies.

TABLE 2: Relative Product Yields from Eq 13 for the Most Reliable Data Sets A3 and B2, Respectively. For the Ozonolysis of TME, the OH Yield Is Set Equal to the Yield of CH_2=$C(CH_3)OOH$ (See Text)

ΔE_{SL}/cm^{-1}	P/mbar	dioxirane	OH	stabilization
Ozonolysis of ethene (set A3)				
250	10.13	0.80	0.0016	0.20
	1013	0.79	0.0016	0.21
500	10.13	0.80	0.0016	0.20
	1013	0.78	0.0016	0.22
	1013	0.71[a]	0.0007[a]	0.29[a]
Ozonolysis of TME (set B2)				
250	10.13	0.047	0.92	0.033
	101.3	0.047	0.89	0.063
	1013	0.044	0.78	0.18
500	10.13	0.047	0.91	0.043
	101.3	0.046	0.84	0.11
	1013	0.040	0.66	0.30
	1013	0.030[a]	0.59[a]	0.38[a]

[a] Zero threshold energy for O_3 + alkene assumed (see text).

When comparing our calculations with experimental results, there are several noteworthy points. The predicted OH yield of ~0.2% under atmospheric pressure seems too low as compared to 12%[17] and 8%[22,24] suggested by experiment. The fraction of stabilized H_2COO is ~20%, where experimental values between 35% and 40% have been determined for atmospheric conditions.[22,24,26,28−30] The measured value for the dioxirane yield of 54%[22,24] differs from the calculated value of 80%. The branching ratio between dioxirane formation and stabilization is reproduced in the correct order of magnitude although its calculated value is larger by a factor of 2. Furthermore, Hatakeyama et al.[27] determined a fraction of 20% stabilized H_2COO at 13 mbar, which agrees with our calculated value at 10 mbar (see Table 2). This low-pressure limiting value corresponds to the fraction of H_2COO that is formed already at energies below the lowest reaction threshold[27] (compare with the hatched area in Figure 4). Hence, this agreement seems to point out that the calculated threshold energy is likely to be correct. The increase of the yield by ~20% in going from 13 to ~1000 mbar, however, is not reproduced by our model. This is due to the high specific rate coefficients for the reaction toward dioxirane, which requires much higher pressures for an effective stabilization to compete (31% at 10 bar, 54% at 100 bar for ΔE_{SL}=500 cm^{-1}). Only a decrease of these rate coefficients by 2 orders of magnitude would approximately

reproduce the above experimental findings. Such a drastic deviation cannot be addressed to possible inaccuracies of the calculated properties of TS6a, which determine the sum of states in eq 14. The reason for these differences in the predicted and measured OH yields is not clear at present.

As was outlined in Section 2, there is a difference of 8 kcal/mol in $\Delta H_f°(298, 7)$ between the CC and the DFT approach. However, this has no influence on the kinetics of the carbonyl oxide, because the disposable energy is determined by the energy difference between TS1 and TS3. The above amount would merely appear in the relative translation of the two fragments H_2CO and H_2COO (cf. Figure 2). To demonstrate the effect of an alteration of the disposable energy, $E^+_{(3)}$, we calculate the product yields for a value that is decreased by 3.5 kcal/mol. The latter is just the threshold energy for the addition step $O_3 + C_2H_4$, and hence the situation considered represents the thermochemical limit between $O_3 + C_2H_4$ and TS3. The results for a pressure of 1013 mbar are contained in Table 2, and one can see that the influence is not very pronounced. The basic features are not changed at all.

We completely neglected in our model the reaction pathway, leading to formaldehyde and $O(^3P)$, which should proceed via intersystem crossing (ISC) to the lowest triplet potential-energy surface and subsequent dissociation. According to Anglada et al.,[25] the configuration of the Criegee intermediate, where ISC is likely to occur, closely resembles that of the transition state for internal rotation around the C−O bond. The threshold energy for the latter process is given as 24.8 kcal mol^{-1}.[25] Thus, apart from the unknown singlet−triplet transition probability, this channel cannot compete with the fast dioxirane formation ($E_0 = 18.2$ kcal mol^{-1}), even though it is energetically accessible for a considerable part of the H_2COO population (cf. Figure 4).

We also did not consider the possibility of a stepwise decomposition of POZ which has frequently been discussed in the literature (for a summary, see ref 44). This is initiated by OO bond cleavage and formation of the biradical •$OOCH_2$-CH_2O•. H migration will lead to the hydroperoxide $HOOCH_2C$-(=O)H, which in turn can decompose to •OCH_2C(=O)H and OH radicals. The activation energy of the first step of this reaction has been estimated to be only a few kcal/mol higher than the cycloreversion step (3) (Figure 1). Hence, it may be possible that OH is also formed in a nonconcerted decomposition reaction, which would explain the fact that in the ozonolysis of ethene more OH was measured than predicted by our calculations. Future work has to clarify this point.

TME + O_3. The average energy of the steady-state population of the primary ozonide under atmospheric conditions is $<E^+_{POZ}>_n = 67.7$ kcal/mol. The resulting rate coefficient for the reaction to the Criegee radical and acetone amounts to 5.6×10^{10} s^{-1}. The collision frequency at 1013 mbar is 1.2×10^{10} s^{-1}, i.e., only by a factor of 4 lower than the rate coefficient. Nevertheless, at this pressure merely 0.04% of the population is stabilized. Assuming an average energy transferred per collision of −300 cm^{-1} (see above), one can estimate that about 40 collisions are required to quench a POZ molecule to an energy range, where it can be considered stabilized ($\omega \approx 10k_3(E)$). This shows the inadequacy of the strong-collision assumption.[49−51]

The disposable energy, $E^+_{(3)} = 54.0$ kcal/mol, is shared on the average as follows: $(CH_3)_2COO$: 28.2, acetone: 23.5, and translation: 2.3 kcal/mol. The nascent population of $(CH_3)_2$-COO as well as the specific rate coefficients for the two reaction pathways are shown in Figure 5. The relative product yields are compiled in Table 2. Here, in contrast to $O_3 + C_2H_4$, the influence of the pressure is much more pronounced, and an adequate modeling of the corresponding tropospheric processes has to account for these effects.

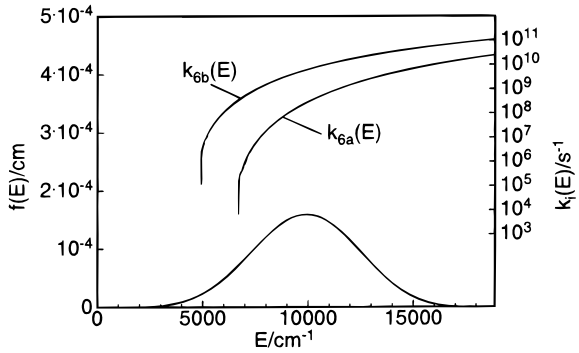

Figure 5. Nascent population of $(CH_3)_2COO$ and specific rate coefficients for the consecutive reactions.

The reaction pathway of $(CH_3)_2COO$ that directly competes with collisional stabilization and formation of dioxirane is the isomerization to CH_2=$C(CH_3)OOH$ (reaction 6b).[13,23] The OH radical, then, is generated in a consecutive step (reaction 8a). Therefore, the question arises, whether the chemically activated hydroperoxide can be stabilized under atmospheric conditions. The corresponding master-equation analysis, eq 13, with an input population from eq 17 and specific rate coefficients from SACM shows that more than 99.99% of the hydroperoxide decompose to give OH and CH_2COCH_3 (average rate coefficient $\sim 4 \times 10^{12}$ s^{-1}). Accordingly, stabilization can be completely neglected. This is in agreement with experimental results.[13] and in contrast to the estimations in ref 14. There is no need for assuming additional reaction pathways such as formation of hydroxyacetone. From our modeling follows that only at pressures as high as 100 bar, stabilization amounts to 1% and at 1000 bar to 12% (with $\Delta E_{SL} = 500$ cm^{-1}).

Compared to experimental investigations, our calculated OH yields of 0.66 and 0.78 (set B2) for step sizes of 500 and 250 cm^{-1}, respectively, are significantly lower than unity[19] and seem to favor the results in the range of 0.7.[13] The fraction of the stabilized Criegee intermediates, between 0.30 and 0.18, is also in reasonable agreement with an experimentally determined value of 0.30.[13] To estimate the influence of the uncertainty of the energy of TS1, i.e., $E^+_{(3)}$, again the limiting case of a zero threshold energy for O_3 + TME is considered. An example for set B2 is also included in Table 2, which confirms that the qualitative picture does not change. In summarizing, our calculations predict under atmospheric conditions a yield of dimethyl dioxirane in the order of 3−5%, an OH yield between ∼60 and ∼80% and a relative fraction of ∼20 to ∼40% for the stabilized dimethyl carbonyl oxide.

Consecutive Reactions of the Stabilized Criegee Intermediate. A further, very important point is the fate of the collisionally deactivated Criegee intermediates, because the above reaction pathways still represent accessible unimolecular channels. Therefore, if the Criegee radicals are not scavenged in a bimolecular step, they will finally undergo the same unimolecular processes with an overall product yield of unity. Even for a completely quenched i.e., *thermal* ensemble at 298 K, one calculates from the high-pressure limiting rate coefficients[49−51] average lifetimes of only 3 s for H_2COO and 0.004 s for $(CH_3)_2COO$, which are drastically below the time scale of most of the experiments performed to investigate the ozonolysis reaction. Moreover, these values represent rather hypothetical upper limits, because the average lifetimes of the intermediates obeying the steady-state distributions are much shorter, viz. $\sim 10^{-9}$ s for H_2COO and $\sim 10^{-7}$ s for $(CH_3)_2COO$.

In ref 22 a combined yield of 47% for CO and CO_2 was measured for O_3 + TME. Our calculated value for dioxirane, however, which should finally yield CO and CO_2, is ~ 5%. On the other hand, the fraction of the stabilized Criegee radical lies in the order of 50%, which seems to indicate a bimolecular reaction of the Criegee intermediate that finally leads to CO an CO_2.

At present the nature of these bimolecular reactions is not quite clear. In experimental studies, mainly SO_2,[27,29] H_2CO,[28,30] HCOOH,[8] and CH_3COOH[8] were used as scavengers, and, moreover, CO, H_2O, NO, and NO_2 are discussed as possible reactants.[1,2,8] Because the corresponding rate coefficients are not known, one might argue that even the choice of the scavenger could influence the yields, especially that for the stabilized Criegee intermediate. For the reaction of H_2COO with O_2, we estimate a rate coefficient of 4.2×10^{-15} cm^3 s^{-1} from our DFT results and simple transition state theory.[63] Because in experimental investigations,[1,22] this reaction was found to be unimportant, the above scavengers should react much faster, especially in view of their usually much lower concentrations in the ppm range. Here clearly additional work is needed. Especially the rate constants of these scavenging processes should be determined to be included in the modeling. Then, also a time-dependent master equation can be used to estimate the quality of the steady-state assumption (eq 10)[54] under atmospheric and smog-chamber conditions.

Despite these open questions, we believe that our model is capable to adequately describe the basic effects of the ozonolysis reactions and, moreover, to predict product yields in an, at least, semiquantitative way. The agreement with experimental results is satisfactory, especially in view of the fact that there were no adjustable parameters used in this work.

Acknowledgment. M.O. wishes to thank the Deutsche Forschungsgemeinschaft (SFB 357 "Molekulare Mechanismen Unimolekularer Prozesse") for financial support. At the University of Göteborg, this work was supported by the Swedish Natural Science Research Council (NFR). Calculations were done on the CRAY YMP/464 and C94 of the Nationellt Superdatorcentrum (NSC), Linköping, Sweden. E. K. and D. C. thank the NSC for a generous allotment of computer time. At the University of Kiel, this work was supported by the CEC within the Environmental Research Program, contract EV5V−CT91−0038.

Supporting Information Available: Cartesian coordinates, rotational constants, and harmonic wavenumbers of all stable molecules and transition states of our systems optimized at B3LYP/6-31G(d,p) level (8 pages). Ordering information is given on any current masthead page.

References and Notes

(1) Finlayson-Pitts, B. J.; Pitts, J. N., Jr. *Atmospheric Chemistry*; Wiley: New York, 1986.
(2) Atkinson, R.; Carter, W. P. L. *Chem. Rev. (Washington, D.C.)* **1984**, *84*, 437.
(3) Greene, C. R.; Atkinson, R. *Int. J. Chem. Kinet.* **1992**, *24*, 803.
(4) Atkinson, R. *J. Phys. Chem. Ref. Data* **1994**, *Monograph 2*, 1.
(5) Grosjean, E.; Grosjean, D. *Int. J. Chem. Kinet.* **1996**, *28*, 911.
(6) Atkinson, R.; Tuazon, E. C.; Aschmann, S. M. *Environ. Sci. Technol.* **1995**, *29*, 1860.
(7) Grosjean, E.; de Andrade, J. B.; Grosjean, D. *Environ. Sci. Technol.* **1996**, *30*, 975.
(8) Neeb, P.; Horie, O.; Moortgat, G. K. *Int. J. Chem. Kinet.* **1996**, *28*, 721.
(9) Japar, S. M.; Wu C. H.; Niki, H. *J. Phys. Chem.* **1976**, *80*, 2057.
(10) Herron, J. T.; Huie, R. E. *J. Am. Chem. Soc.* **1977**, *99*, 5430.
(11) Herron, J. T.; Huie, R. E. *Int. J. Chem. Kinet.* **1978**, *10*, 1019.
(12) Martinez, R. I.; Herron, J. T.; Huie, R. E. *J. Am. Chem. Soc.* **1981**, *103*, 3807.
(13) Niki, H.; Maker, P. D.; Savage, C. M.; Breitenbach, L. P.; Hurley, M. D. *J. Phys. Chem.* **1987**, *91*, 941.
(14) Martinez, R. I.; Herron, J. T. *J. Phys. Chem.* **1987**, *91*, 946.
(15) Martinez, R. I.; Herron, J. T. *J. Phys. Chem.* **1988**, *92*, 4644.
(16) Atkinson, R.; Hasegawa, D.; Aschmann, S. M. *Int. J. Chem. Kinet.* **1990**, *22*, 871.
(17) Atkinson, R.; Aschmann, S. M.; Arey, J.; Shorees, B. *J. Geophys. Res.* **1992**, *97*, 6065.
(18) Paulson, S. E.; Flagan, R. C.; Seinfeld, J. H. *Int. J. Chem. Kinet.* **1992**, *24*, 103.
(19) Atkinson, R.; Aschmann, S. M. *Environ. Sci. Technol.* **1993**, *27*, 1357.
(20) Horie, O.; Neeb, P.; Moortgat, G. K. *Int. J. Chem. Kinet.* **1994**, *26*, 1075.
(21) Gutbrod, R.; Rahman, M. M.; Schindler, R. N. *Air Pollution Res. Report* **1994**, *54*, 133.
(22) (a) Gutbrod, R.; Meyer, S.; Rahman, M. M.; Schindler, R. N. *Int. J. Chem. Kinet.* **1997**, *29*, 717. (b) Gutbrod, R. *Dissertation*, Kiel, 1996.
(23) Gutbrod, R.; Schindler, R. N.; Kraka, E.; Cremer, D. *Chem. Phys. Lett.* **1996**, *252*, 221.
(24) Gutbrod, R.; Kraka, E.; Cremer, D.; Schindler, R. N. *J. Am. Chem. Soc.* **1997**, *119*, 7330.
(25) Anglada, J. M.; Bofill, J. M.; Olivella, S.; Solé, A. *J. Am. Chem. Soc.* **1996**, *118*, 4636.
(26) Hatakeyama, S.; Kobayashi, H.; Akimoto, H. *J. Phys. Chem.* **1984**, *88*, 4736.
(27) Hatakeyama, S.; Kobayashi, H.; Lin, Z.-Y.; Tagaki, H.; Akimoto, H. *J. Phys. Chem.* **1986**, *90*, 4131.
(28) Niki, H.; Maker, P. T.; Savage, C. M.; Breitenbach, L. P. *J. Phys. Chem.* **1981**, *85*, 1024.
(29) Su, F.; Calvert, J. G.; Shaw, J. H. *J. Phys. Chem.* **1980**, *84*, 239.
(30) Kan, C. S.; Su, F.; Calvert, J. G.; Shaw, J. H. *J. Phys. Chem.* **1981**, *85*, 2359.
(31) Cremer, D. *J. Am. Chem. Soc.* **1981**, *103*, 3619, 3627, 3633.
(32) Cremer, D. *Angew. Chem.* **1981**, *93*, 934; *Int. Ed. Engl.* **1981**, *20*, 888.
(33) Cremer, D.; Kraka, E.; McKee, M.; Radhakrishnan, T. P. *Chem. Phys. Lett.*, **1991**, *187*, 491.
(34) Cremer, D.; Gauss, J.; Kraka, E.; Stanton, J. F.; Bartlett, R. J. *Chem. Phys. Lett.* **1993**, *209*, 547.
(35) Kraka, E.; Cremer, D. to be published.
(36) (a) Becke, A. D. *J. Chem. Phys.* **1993**, *98*, 5648. (b) Stevens, P. J.; Devlin, F. J.; Chablowski, C. F.; Frisch, M. J. *J. Phys. Chem.* **1994**, *98*, 11623. (c) Bauschlicher Jr., C. W.; Partridge, H. *Chem. Phys. Lett.* **1995**, *240*, 533.
(37) Hariharan, P. C.; Pople, J. A. *Chem. Phys. Lett.* **1972**, *66*, 217.
(38) See for example: (a) Jones, R. O.; Gunnarsson, O. *Rev. Mod. Phys.* **1989**, *61*, 689. (b) Kristyan, S.; Pulay, P. *Chem. Phys. Lett.* **1994**, *229*, 175. (c) Andersson, Y.; Langreth, D. C.; Lundquist, B. I. *Phys. Rev. Lett.* **1996**, *76*, 102. (d) Johnson, B. G.; Gonzales, C. A.; Gill, P. M. W.; Pople, J. A. *Chem. Phys. Lett.* **1994**, *221*, 100. (e) Baker, J.; Andzelm, J.; Muir, M.; Taylor, P. R. *Chem. Phys. Lett.* **1995**, *237*, 53. (f) Jursic, B. S. *J. Chem. Soc., Perkin Trans. 2* **1997**, 637.
(39) Kraka, E.; Gauss, J.; Reichel, F.; Olsson, L.; Konkoli, Z.; He, Z.; Cremer, D. *COLOGNE 94*, Göteborg, 1994.
(40) Frisch, M. J.; Head-Gordon, M.; Trucks, G. W.; Foresman, J. B.; Schlegel, H. B.; Raghavachari, K.; Robb, M. A.; Binkley, J. S.; Gonzalez, C.; Defrees, D. J.; Fox, D. J.; Whiteside, R. A.; Seeger, R.; Melius, C. F.; Baker, J.; Martin, R. L.; Kahn, L. R.; Stewart, J. J. P.; Topiol, S.; Pople, J. A. *Gaussian 92*; Gaussian Inc.: Pittsburgh, 1992.
(41) Stanton, J. F.; Gauss, J.; Watts, J. D.; Lauderdale, W. J.; Bartlett, R. J. *ACES II*, Quantum Theory Project: University of Florida, 1992.
(42) (a) Chase, Jr., M. W.; Davies, C. A.; Downey, Jr., J. R.; Frurip, D. J.; McDonald, R. A.; Syverud, A. N. *J. Phys. Chem. Ref. Data*, **1985**, *14*, Suppl. 1. (b) See also: McMillen D. F.; Golden, D. M. *Annu. Rev. Phys. Chem.* **1982**, *33*, 493.
(43) Gillies, C. W.; Gillies, J. Z.; Suenram, R. D.; Lovas, F. J.; Kraka, E.; Cremer, D. *J. Am. Chem. Soc.* **1991**, *113*, 2412.
(44) Bailey, P. S. *Ozonation in Organic Chemistry*; Vol. 1 and 2, Academic Press: New York, 1978 and 1982.
(45) Raghavachari, K.; Trucks, G. W.; Pople, J. A.; Head-Gordon, M. *Chem. Phys. Lett.* **1989**, *157* 479.
(46) (a) Dunning Jr., T. H. *J. Chem. Phys.* **1970**, *53*, 2823. (b) Dunning Jr., T. H. *J. Chem. Phys.* **1971**, *55*, 716. (c) For the polarization exponents, see: Redmon, L. T.; Purvis G. D.; Bartlett, R. J. *J. Am. Chem. Soc.* **1979**, *101*, 2856.
(47) He, Z.; Yuan, H.; Cremer, D. *Chem. Phys. Lett.*, in press.
(48) Harding, L. B.; Goddard, W. A. *J. Am. Chem. Soc.* **1978**, *100*, 7180.
(49) Robinson, P. J.; Holbrook, K. A. *Unimolecular Reactions*; Wiley: New York, 1972. Holbrook, K. A.; Pilling, M. J.; Robertson, S. H. *Unimolecular Reactions*, 2nd ed.; Wiley: Chichester, 1996.

(50) Forst, W. *Theory of Unimolecular Reactions*; Academic Press: New York, 1972.

(51) Gilbert, R. G.; Smith, S. C. *Theory of Unimolecular and Recombination Reactions*; Blackwell: Oxford, 1990.

(52) Rabinovitch, B. S.; Diesen, R. E. *J. Chem. Phys.* **1959**, *30*, 735; Rabinovitch, B. S.; Kubin, R. F.; Harrington, R. E. *J. Chem. Phys.* **1963**, *38*, 405.

(53) Hoare, M. *J. Chem. Phys.* **1963**, *38*, 1630.

(54) Schranz, H. W.; Nordholm, S. *Chem. Phys.* **1984**, *87*, 163.

(55) Olzmann, M.; Gebhardt, J.; Scherzer, K. *Int. J. Chem. Kinet.* **1991**, *23*, 825.

(56) Reid, R. C.; Prausnitz, J. M.; Poling, B. E. *The Properties of Gases and Liquids*; McGraw-Hill: New York 1987.

(57) Snider, N. *J. Chem. Phys.* **1985**, *89*, 1257.

(58) Oref, I.; Tardy, D. C. *Chem. Rev. (Washington, D.C.)* **1990**, *90*, 1407. Hippler, H.; Troe, J.; Wendelken, H. J. *J. Chem. Phys.* **1983**, *78*, 6709. Rossi, M. J.; Pladziewicz, J. R.; Barker, J. R. *J. Chem. Phys.* **1983**, *78*, 6695.

(59) Press: W. H.; Flannery, B. P.; Teukolsky, S. A.; Vetterling, W. T. *Numerical Recipes*; Cambridge University Press: Cambridge, 1989.

(60) Marcus, R. A.; Rice, O. K. *J. Physic. Colloid Chem.* **1951**, *55*, 894. Marcus, R. A. *J. Chem. Phys.* **1952**, *20*, 359.

(61) Beyer, T.; Swinehart, D. F. *Comm. Assoz. Comput. Mach.* **1973**, *16*, 379. Astholz, D. C.; Troe, J.; Wieters, W. *J. Chem. Phys.* **1979**, *70*, 5107.

(62) Quack, M.; Troe, *J. Ber. Bunsen-Ges. Phys. Chem.* **1974**, *78*, 240. Troe, J. *J. Chem. Phys.* **1983**, *79*, 6017.

(63) Glasstone, S.; Laidler, K. J.; Eyring, H. *The Theory of Rate Processes*; McGraw-Hill: New York, 1941. Steinfeld, J. I.; Francisco, J. S.; Hase, W. L. *Chemical Kinetics and Dynamics*; Prentice Hall: Englewood Cliffs, 1989.